Paper V

Image-Analytical Quantitative Monitoring of Heterogeneous Mixture Processes: Angle Measure Technique (AMT) vs. Multivariate Image Regression (MIR)

Thorbjørn Tønnesen Lied, Inger Hedvig Matveyev,
Dawn Angela Field Karlsrud, Jun Huang and Kim H. Esbensen*

Applied Chemometrics Research Group (ACRG), Department of Technology (TF)
Telemark University College (HiT), N-3918 Porsgrunn, Norway

* Corresponding author. E-mail: kim.esbensen@hit.no

CONTENTS

ABSTRACT

Selected two- and three-component mixtures are studied by image analysis plus *chemometric data analysis*, specifically AMT (Angle Measure Technique), MIR (Multivariate Image Analysis - and the recent extension termed MIR^{+}) and PLS-R (Partial Least Squares Regression). The present studies comprise a first foray regarding the possibilities of continuous mixing process - and product monitoring (homogeneity, on-line mixing fraction quantification etc.) using image analysis as the primary data capture facility.

We study three very different types of mixing systems, i.e. dry two-component powder systems, frozen three-component vegetable mix systems and a minced meat mixing system - the latter two of which constitute real-world industrial systems of current economical interest.

Results show that the present line-up of chemometric image analysis and data analysis methods are fully sufficient to outline a framework for automated process monitoring systems. The two-component systems are also representative of a much larger study (barely initiated) on the possibilities of predicting the ultimate propensity of mixing systems, based only on standard image analysis characterisation *plus* the necessary chemometric data analysis.

We conclude that *both* the AMT and the MIR^{+} approaches are suitable for the realistic tasks specified in the current studies, both with satisfactory relative prediction accuracies and precisions as estimated from comparable cross-validations.

INTRODUCTION

Mixing, blending, homogenisation of granular poly-component materials is of great importance in modern manufacturing and in large-scale process industries. These processes have been studied intensively within the field of powder science and technology. Despite it's importance, however, a full understanding of granular mixing processes is surprisingly limited. Often quite unexpected segregation can occur, even in what was thought to be well-designed mixers or blenders, for example when batches are mixed just slightly "to fast" or for just a trifle "too long" etc. A recent overview highlighted these difficulties graphically with great impact[1]. Here was outlined in detail the many factors involved in determining the ultimate outcome of a particulate matter mixing. We have determined to begin a major effort of mapping the interplay between these instrumental factors - only based on a direct image analysis characterisation of the components involved plus whatever *a posteriori* intricate (or

simple) data analysis needed. I.e. we want to find out the possibilities - and limitations - of being able to use only a standard, non-invasive image analysis recording technique of the *in-situ* appearances of the end-member components involved - in order to be able *to predict* the final outcome of physical mixing- and blending testing under real-world conditions (this latter to be carried out in realistic full-scaled certified mixing experiments of the type reported in [1]). For this predictive effort, as well as for the presumably rather complex post-imaging data treatment necessary, we turn to *chemometrics*, which has been used in connection with powder science and technology only in the last five years, but with rather spectacular results [2, 3, 4 , 5, 6].

As a first side-benefit of the above major experimental research program it was found that a selected few of the many types of poly-component mixtures involved, also could serve a more limited purpose of illustrating new, modern and efficient possibilities for on-line mixing process characterisation, together with a few different, but closely related, types of mixtures, all of which have very great significance as general representatives of industrial systems in need of reliable, precise and accurate process monitoring (mixing process monitoring). On the market today there are to be found many types of such monitors to be sure, but they are all more-or-less rather dedicated systems directed towards rather narrow classes of materials, powders etc.

We want to develop a completely *generic* image analysis_cum_chemometrics system, to be based on existing, inexpensive off-the-shelf digital video camera technologies only. Thus the "new" elements in the system we are developing will mainly be the problem-specific chemometric image data analysis (AMT, MIR^{+}) and related quantitative prediction facilities involved (PLS). We shall use very simple digital video imaging data capture in our studies, which never-the-less is of exact industrial standards.

Specifically the present work attempts to predict quantitative mixing fractions on a selected set of (very) different mixing series. We *simulate* on-line monitoring of representative mixing processes, by preparing precise (v/v %) quantitative fractions of the granular materials involved and subjecting them to the above camera under direct industrial process monitoring conditions.

Of the methods employed here, the Multivariate Image Regression (MIR) approach is used to establish a relationship between video imagery data (X) and functional granular properties (Y) (here we limit ourselves to addressing quantification of the homogeneity of mixings, but in the major research program mentioned above, we shall also address

a range of other, standard powder characterising functional properties). Images taken of granular materials are bound to contain inherent information concerning the geometric shape(s) of the individual particles, their sizes, or size distributions, surface roughness, irregularities, smoothness, etc. This type of imagery will also contain information related to the ensemble of particles, to the particulate aggregate, or powder etc. as it were. Both these basic types of characteristics can be related to the bulk granular functional properties and mixing fractions, using proper *multivariate calibration* (PLS-regression), based on derived AMT-spectra[2] and/or MIR analysis techniques [8-9]. The major methodological objective of the present work will be to *compare* these fundamental two (the AMT-based and the MIR-based) prediction possibilities.

Two laboratory systems are studied below, a selected suite of four dry two-component powder systems (representing very varying colour -, reflectance -, as well as morphological contrast) and a system consisting of vegetable mixes of three end-components. The first set is used to study the more fundamental factors governing the mixing processes and - results, while the second set is a *bona fide* industrial mixing process monitoring example.

In addition to this study of granular mixtures, a real-world food mixing process involving minced meat (mincing meat and fat at industrial scales) is examined, using a newly developed industrial standard mixer ("IDE-CON"). To be able to satisfy their customers, producers of minced meat products are critically dependent upon reliable, essentially real-time on-line measurements of fat content in their products, as only very small deviations from the health authority specifications are accepted. Traditional off-line fat measurements are time-consuming and certainly not continuous. Image analytical on-line measurements would be very preferable, if feasible, also because of the possibility of actually designing systems with an ability - in principle - to be *totally representative*, i.e. image analysis solutions have the prospect of being able to inspect the *entire* production output.

A few examples of *sample preparation problems* occurred when certain sample types were introduced to the camera. Homogeneous mixtures would sometime *segregate* slightly when being poured onto the sample presentation plate in front of the camera etc. Flow - and transportation segregation is often a well-known problem in the handling of particulate matter. We made serious efforts to curtail this heterogeneity-increasing factor in the studies presented below, by *standardising* the specific sample presentation process (presenting the sample to the camera) throughout. On the other

hand what (little?) *pouring segregation* variance remaining was accepted as it indeed mimics correctly the identical problem facing industrial inspection systems. This certainly introduced more realistic variation in the analysis results obtained over that of otherwise "idealised" laboratory systems.

AMT (Angle Measure Technique)

The AMT transform, as a new *signal analysis* method, has shown potential in many areas of science and technology since its debut in 1994. It characterises the scale-dependent complexity of data such as time series, spatial data series, indeed any generic *measurement series*, in a new domain - the *scale domain*. Applications include image analysis, signal analysis, spectroscopy, analysis of drilling well log data, measurement runs in quality control, etc [2-6].

AMT has been applied on powder imagery in connection with multivariate calibration in a series of recent studies resulting from our chemometric collaborations in powder science and technology [2-6]. AMT has shown a significant positive propensity as a salient *pre-processing* facility for quantifying the textural characteristics of images. When derived AMT-spectra (see further below) are subjected to *multivariate calibration*, e.g. in the form of PLS-regression modelling, a combined facility termed MAR (Multivariate AMT Regression) has been shown to have a very wide applicability. It is especially the combined facility of being able to quantify texture features for both individual particles as well as for their aggregate (powder/mixture) characteristics which comes to the fore in these applications, allowing for materials characteristication *simultaneously over all particulate scales*.

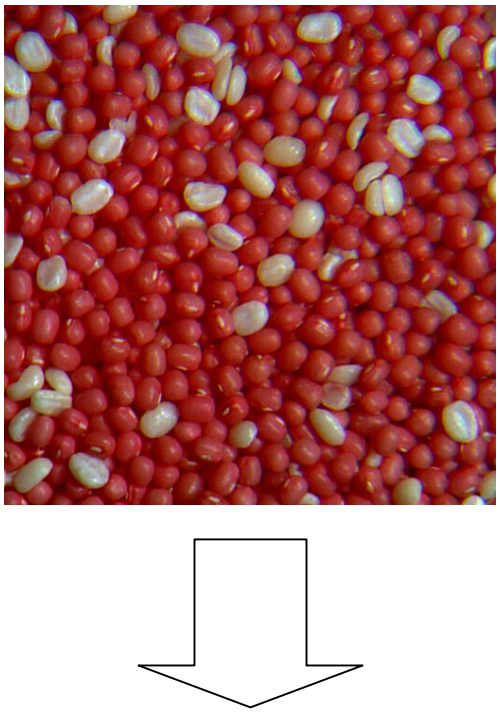

Figure 1. A representative image of a mixture of particulate matter, to be unfolded *and subjected to AMT-characterisation*

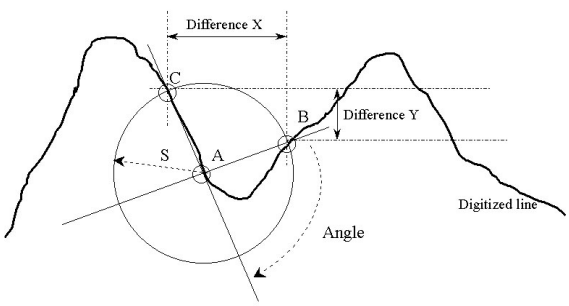

Figure 2. AMT-derivation of the so-called MA angle measure (Mean Angle). The extensive reference litterature explains parallel derivation of the MDY-measure as well [2-6].

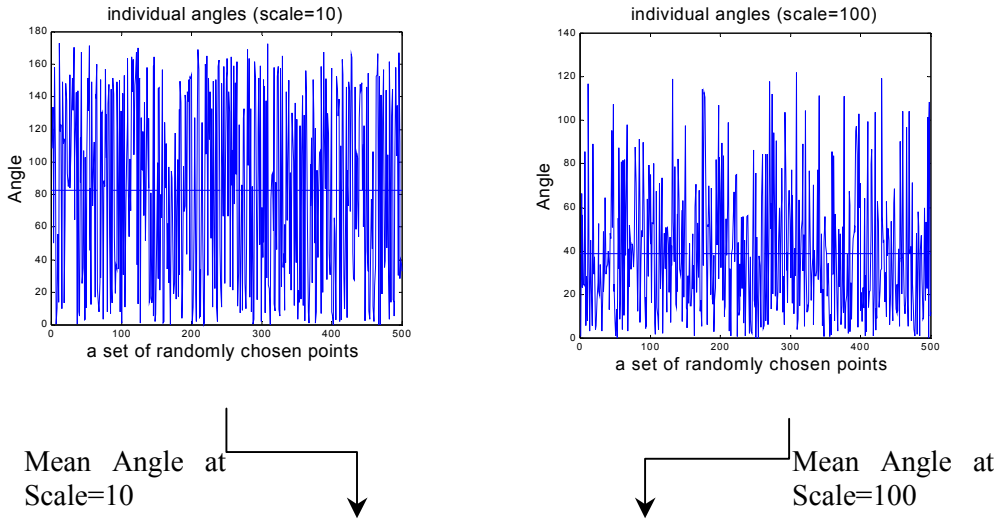

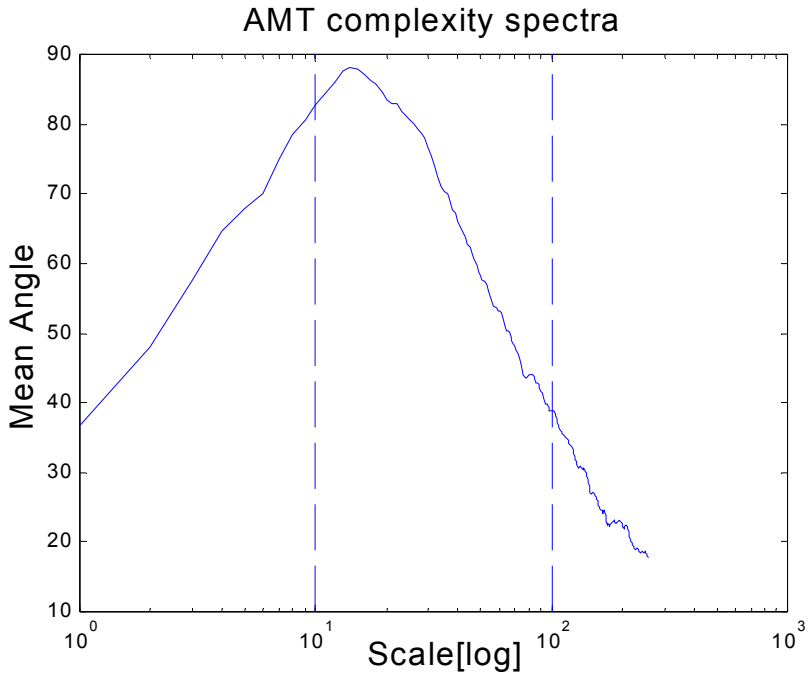

Figure 3. Illustration of representative AMT complexity-spectrum derived from a mixture image. Observe how the MA-spectrum is calculated as the mean of all individual angle measures at all scales, two of which two have been highlighted (scales = 10, 100). The horizontal axis represents "log S". MA displays a complexity "peak" corresponding to a scale of approx. 10-30. When several AMT-spectra are collected into a common X-matrix, the (log S) scale is used as the variable dimension. For full details of AMT [2-6].

The most useful aspect of the AMT transform is that the compound (**MA**, **MDY**) spectrum can be used as 1-D object vectors in multivariate data modelling (e.g. PCA or PLS). For 2-D image objects it is the *local texture* of the field-of-view which is transformed into a corresponding 1-D *linear complexity spectrum*. These complexity spectra, implicitly carry a remarkable information richness related to all scale(s).

Multivariate AMT regression (MAR) has brought a new approach to extracting information for prediction purposes from "measurement series" (of any kind), which in the present context consist of *unfolded*[†] isotropic digital images. This approach converts texturally isotropic images into 1-D multivariate AMT-spectra without loss of fidelity. It views an image in a mathematically transformed way instead of by direct visualization. The present work deals with granular powder and food particular materials as well as minced meat imagery, but applies equally well in many other similar situations.

Figure 4 below shows a schematic overview of the processes involved when using AMT-spectra of images for multivariate calibration. The MAR approach requires several steps when used for quantification of heterogeneous mixtures. Regression models must either be created based on images of *pure* mixing-components (classes), or based on a series of "spiked" concentrations of one, or more of the end-member fractions etc. The appropriate AMT-spectra are combined in a training data set related to the multivariate calibration PLS-modelling. If possible a relevant test set should also be prepared etc [7].

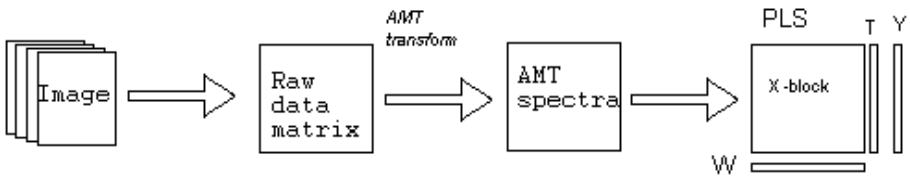

Figure 4. Schematic overview of image processing with AMT before regression calibration, MAR (Multivariate AMT Regression).

[†] *Unfolded* is here used to describe the operation of rearranging each image-channel from a 2D matrix to a long 1D vector.

For a full description of the AMT approach, see [2-6]. Suffice here to emphasise that the AMT image processing approach deals with characterisation of *contrasts* in both colour, reflectance, texture, individual grain forms and more. Thus it is not only the - perhaps more conventional - geometrical texture interpretations which are codified. Since derived AMT-spectra of an imaged material represent a *unique* scale-domain complexity/texture pattern of the image, they are well suited for calibration of images where *changes in overall texture* is an issue. Consider e.g. a series of fractions of two -, three - (or poly-) component mixtures (used as a calibration data set for the present studies). It will be seen that it is the *totality* of all these potential texture features which is changed when the mixing fractions of one (or more) of the end-members are changed. This shall be amply illustrated below. It bears to observe that it is not strictly necessary to be able to understand in all details which of the *individual* different contrasting texture factors are involved - nor *how*, or their supposed much more complex potential *interactions*. We have shown in several of the precursor investigations upon which the present work is firmly established [2-6], that the compound AMT-spectra in a sense *automatically* codifies all relevant factors and that it is the subsequent PLS-regression multivariate calibration which is responsible for extraction of *precisely* those parts of these X-spectra which *correlates* most strongly to the chosen Y-variable, which will be the pertinent mixing-fractions in all present studies.

There is thus a well-reflected reason to expect that the AMT- approach also will be successful in quantifying the mixing-fractions involved in the present experiments, but it is an open question to what ultimate levels of accuracy and precision this will be attainable. The AMT-approach will be compared below with the Multivariable Image Regression alternative, MIR - especially in a novel, extended modification, MIR^{+}.

The MIR Concept

MIR (Multivariate Image Regression) [8, 9, 10, 11] can also be viewed as a transformation of images. In this case, the multivariate image is transformed from raw data to PLS-components [12, 13, 14] called *score-images*. MIR is aimed towards being able to predict Y-images based on a regression model [15, 16, 17]. The predicted images may often constitute the final result in themselves, but can also sometimes be used for further feature extraction in several ways.

The MIR approach requires several steps when used for quantification of heterogeneous mixtures. First of all, regression models should be created from images

of *pure* mixing-components (classes). These images are combined in a training data set, as shown in Figure 5.

In this illustration three models are created, one for each class. It is possible to use PLS2 to create one general model for all classes, but predictions will usually be improved by using separate models [7]. Appropriate reference Y-images are generated so as to maximise the grey-level intensity differences between the end members. The Y-image contains the maximum grey-level value at the image positions of the training object(s), and the minimum values in all other positions. For an unsigned, 8-bit image these values are 255 (white) and 0 (black), respectively. The graphic illustration in Figure 5 is probably much more directly telling....

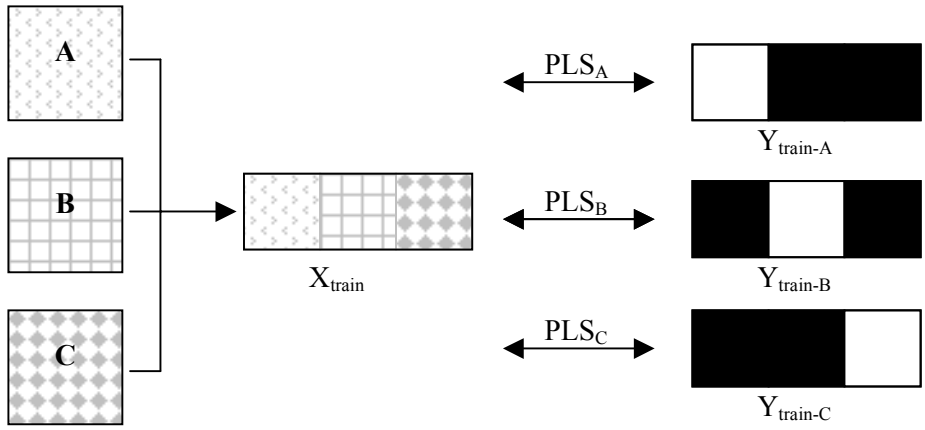

Figure 5. Illustration of MIR training set-up for quantitative characterisation of classes A, B and C of heterogeneous mixtures. A separate model is calibrated for each class, using dichotomous (white/black) reference Y-masks.

When acquiring *new images* of mixed classes - corresponding to taking an image of the product to be characterised (f. ex. on the production conveyor belt etc.), these will be Y-predicted with the models created above. If the training models have been created successfully, and if the particular input-output relation is generally linear or can be modelled by a bilinear PLS-regression model, pixels belonging to the current training class in question will be characterised by bright grey-level values ("close to white"), while all other pixels will usually be much more dark in their grey-level values. The fraction of "bright pixels", suitably defined (problem-dependent), will thus be expected to correlate to the overall mixing-fraction of the *current class* in the mixture. We have recently published several extensive MIR descriptions with a wide variety of laboratory and industrial illustrations elsewhere; see [8-17] for in-depth MIR coverage.

While AMT mainly focuses on textural and spatial information like contrasts in shape and pattern, MIR focuses on *spectral information*. This means that AMT has its preferences if texture and spatial information is important, while MIR relies much more on differences in colour etc. with which to classify and to quantify objects. It is thus expected that it is not necessarily an easy given which method to apply in a given situation. Clearly one needs a lot of experience with many, and diverse, problem-dependent data sets and applications. If both spectral and spatial information is valuable for the quantification, *combining* the results from AMT and MIR should be an advantageous possibility.

Analysing the primary MIR prediction results

Three different approaches are discussed when it comes to correlating the MIR-predicted images with the concentrations of the different mixing fractions. Two of these are univariate, and the third method is based on multivariate calibration.

Thresholding

Thresholding is perhaps the most well-known “traditional” way of analysing the frequency of bright pixels in an image. By converting the image to black and white at some critical grey-level *threshold-value* and then counting the number of "white pixels", an estimate of the concentration of the class can be calculated. If the black and white image is binary (0’s and 1’s), calculating the *mean value* will give the mixing-fraction directly.

Problems with this approach applies to noise in the data that f. ex. may result from sub-optimal lighting conditions (highlights and/or shadows), which can lead to severe misclassification etc.

The Mean Grey-level Value

Especially when dealing with two-component mixtures, in which one end-member is predicted bright and the other dark, calculating the *mean grey-level value* will correlate to the fraction of bright pixels in the image. This method does not give an answer in fractions units though, and some further (linear) adaptation of the result will be required.

Histogram Calibration - Extended MIR (MIR$^+$)

Instead of thresholding, or calculating a mean grey-level value for the image, the entire grey-level histogram[18] of the predicted image can be used for multivariate calibration

using PLS. This approach is the one most similar to the AMT approach, which also depends on multivariate calibration of (complexity) spectra. Figure 6 shows how MIR and 2-way PLS relates to the multivariate image **X**, the predicted $\hat{\mathbf{Y}}$-image and its histogram. The MIR model being used for $\hat{\mathbf{Y}}$-prediction has been established earlier using the approach outlined in Figure 5. The PLS-model used to predict the final mixing fractions has been established on the basis of a calibration set of several histograms with known Y-values. This is in fact a standard 2-way PLS multivariate calibration, in which the initial MIR Y-image prediction_cum_histrogram derivation can be viewed as an image pre-processing step.

This new *compound* MIR/Y-pred/histogram/PLS-approach is termed the ***extended*** MIR: MIR^{+}.

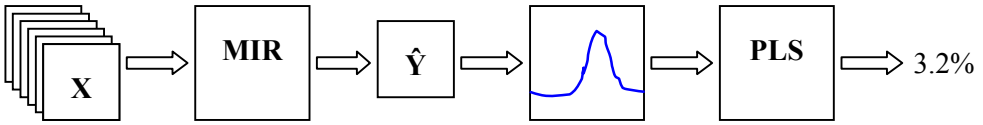

*Figure 6. The MIR^{+} $\hat{\mathbf{Y}}$-histogram prediction approach. A $\hat{\mathbf{Y}}$-image is predicted from the Multivariate Image **X** using an existing MIR model. The histogram of the $\hat{\mathbf{Y}}$-image grey-levels is used for training a traditional 2-way PLS-R model.*

It might perhaps be argued that instead of predicting an image prior to mixing fraction calibration, why not just use the raw image grey-level histograms directly? In some simple cases this *may* indeed be possible, but certainly not as a general approach. When working with a large number of video channels, it can be seen generally to be difficult to isolate just one *singular* channel that optimally enhances a single class with respect of all other classes, compare above. The powerful data compression that lies in MIR (PLS), and the extended MIR^{+}, is most often much more effective for extracting the kind of information needed for the calibration of a specific class or for quantitative mixing fraction prediction.

DATA PRESENTATION

AMT and MIR has been applied in parallel to all the data sets presented briefly in the introduction above. The data sets are further presented in a sufficient detail below - with representative imagery and accompanying explanations - in order to be able to serve as the common framework for *comparing* the alternative AMT and MIR^{+} quantifications below.

Three different mixing product types were used: two-component dry granular mixtures, three-component "wet" mixture and three different series involving mixing fat into minced meat product types.

Two-Component dry Granular Mixtures

Four representative combinations of two-component granular mixtures was selected for the present purpose - out of a significantly larger *experimental design* of nine mixing series, which have been designed to span a maximum coverage w.r.t. the three principal design variables: *colour* contrast; *reflectance* contrast and *morphological* contrast. (These design variables represent critical material factors involved in image analytical imagery, representing the primary image quality response(s) to the illumination conditions etc.). This background study specifically only addresses the AMT-prediction feasibility studies.

The four series chosen here represent both "easily AMT-modelled" systems, as well as their *distinct counterparts*, i.e. systems which did not lend themselves to fair AMT-modelling - perhaps potential candidates for the alternative MIR^{+} approach?

The first dry two-component mixture consists of whole-grain black pepper and white PVC-pellets, generally of similar grain size, Figure 7. This mixture was chosen because of its marked high spectral - (large colour difference) and textural contrasts (relatively large difference in grain form definitions). The data set contains 11 principal mixing fractions, all imaged with *four replicates*. For one component the fraction was [0%, 10%, 20%, …, 100%], with complementary fractions for the other.

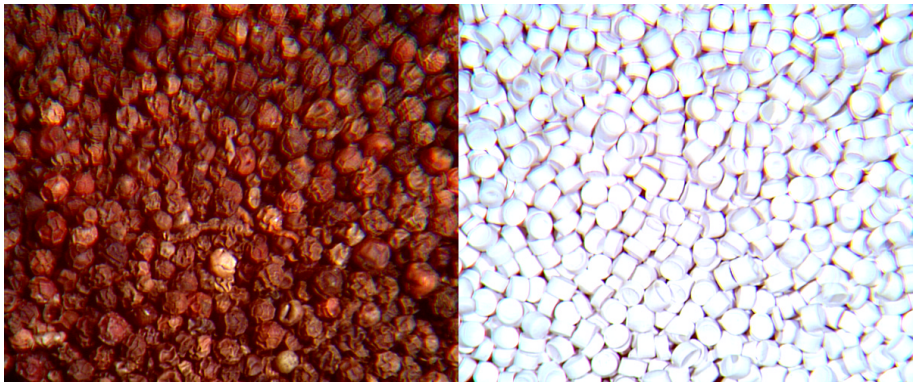

Figure 7. Whole-grain black pepper and white PVC-pellets. Training set-up of pure classes.

The second dry granular mixture involved a *whole-grain* coriander and *ditto* white pepper mixture, illustrated below. This system was chosen as a "maximally difficult

system". Thus a mixing system was deliberately *designed* to have maximally low spectral and textural, as well as morphological contrast for both end-members, i.e. In Figure 8 one observes the dramatic difference to the system in Figure 7. In this system it is decidedly not easy to distinguish between the individual grains from either pure end-member.

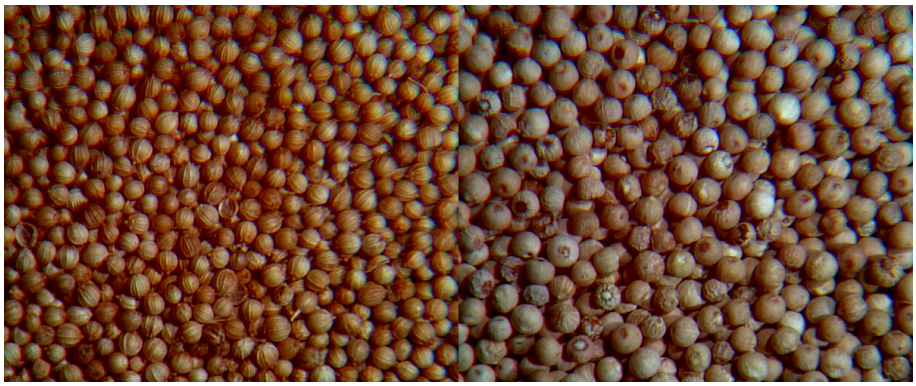

Figure 8. Whole-grain coriander (left) and ditto white pepper (right). Observe the dramatically smaller contrast compared with Figure 7.

The additional two dry mixture systems were chosen so as to represent more intermediate contrast ranges for the three design factors.

The third two-component mixture thus concerned grey and white PVC-pellets, Figure 9 with relatively high spectral contrast, but distinctly low textural contrast. There are however some important differences w.r.t. the individual grain shapes, but their average grain sizes are almost equal. Compared with Figure 7 & Figure 8, this system is clearly intermediary, as is it's close companion, shown in Figure 10 (the same grey PVC-pellets, but now mixed in with green beans).

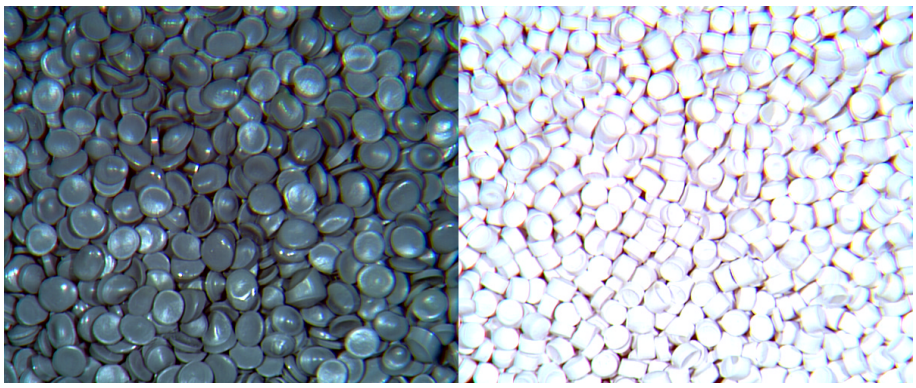

Figure 9. Grey and white PVC-pellets (of different grain shapes)

The last two-component mixture (grey PVC-pellets/green beans), Figure 10, was chosen primarily for the marked (large) contrast w.r.t. to the two individual grain shapes involved - every other contrast being in the intermediary/low range.

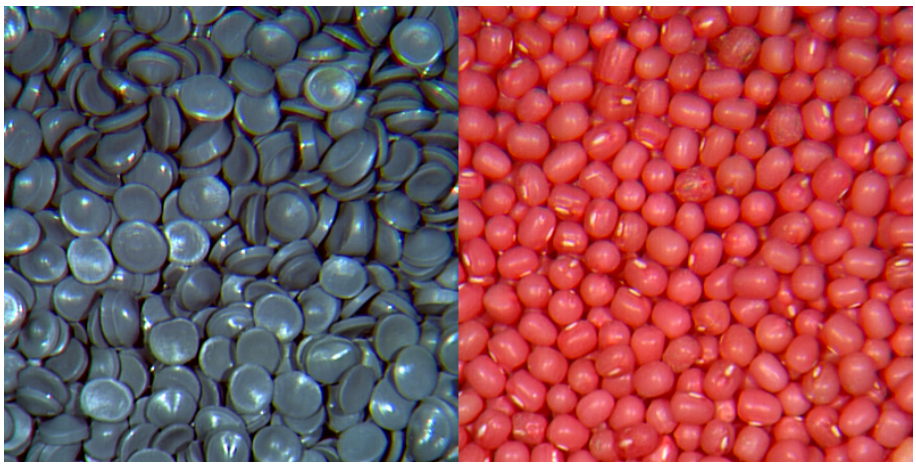

Figure 10. Grey PVC-pellets (left) and green beans (right). The NIR-Red-Green camera used (SILVACAM) is responsible for the false colour appearance of the "green" beans in this rendition. Note especially high grain shape/form contrast.

Three-Component Granular Mixtures

One major three-component example was selected for this study, a real-world industrial mixing problem directly from the production line of a Norwegian producer of vegetable mixes - in the present example we focused on an *evergreen* mix: green peas/maize/carrot (cubes), Figure 11. The producer is concerned with on-line quality control (just precise enough), which translates into an image analysis system, which should be able to predict mixing fractions of two of the three components with a precision of 8% (rel.) or better. In the laboratory experimental design used here, the fractions of each component was varied in increments 0%, 25%, 33%, 50%, 67% 75% or 100%. The imaging system is presented below, Figure 17.

For this three-component system we experienced occasional rather severe homogenisation -, and especially critical *pouring segregation* when presenting the mixed samples to the camera field-of-view, compare above ("Introduction"). It was necessary to instigate a detailed sample handling and presentation protocol, to be very strictly adhered to for all samples involved - and still some measure of residual individual sample preparation variance could be observed. This we decided to keep as it was however, for reasons of compliance with realistic on-line sample preparation in the industrial realm.

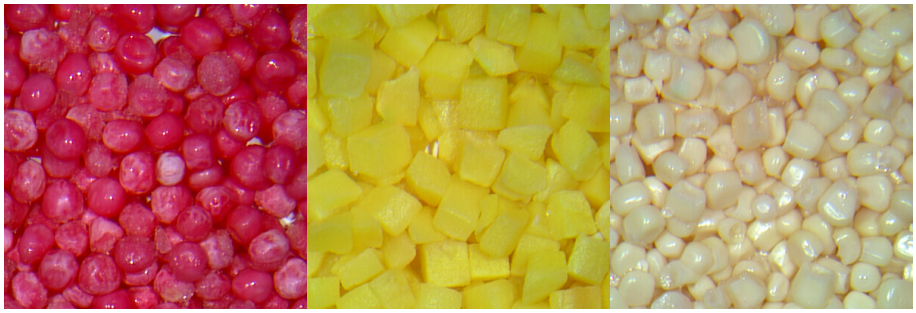

Figure 11. Green peas (left), carrot (middle) and maize (right) pure training classes(100%) respectively . SILVACAM's false colours figures prominently here, but are of no consequence for the spectral contrasts involved.

On-line Minced Meat Mixing Fraction Specification Control

Applied Chemometric Research Group is presently involved in a long-term campaign of particulate matter and powder application studies. One recent new avenue concerns outlet quality control from a novel industrial mixer (the "IDE-CON" mixing concept), which is briefly presented in Figure 12.

Figure 12.The IDE-CON continuous mixer. Note the two counter-rotating shovels of the new, proprietary IDE-CON design.

The IDE-CON continuous mixer is presently used extensively in selected test industrial sectors, amongst which mentioning of the following high-precision target examples should suffice to illustrate the importance a reliable mixer-outlet product specification

verification: on-site road tarmac mixing/blending from three raw materials (all at elevated temperatures of about 85°C; several poly-component health product manufacturing, with up to 10 components in concentrations ranging from, say 1000 ppm to typical filler status (50-90%).

The IDE-CON mixer has the added versatility of being able of *continuous* on-line *adjustment* of the blending/mixing regimens as needed. Therefore it is also used in industrial sectors and branches, for example the food - and feed producers etc. where non-invasive (indeed sterile), strongly regulated, precise control facilities are required by the authorities. As an example, from a leading Norwegian agricultural producer, our last example is related to industrial production of minced meat products - in which quick adjustment of the mixer is often required, (virtually instantaneous changes in the current product specifications). Three different meat + fat mixture series was studied directly in the IDE-CON mixer: bovine meat vs. fat (Figure 13), pork vs. fat (Figure 14) and (bovine + pork) vs. fat (Figure 15). The fat fraction to be added varied from 22% to 42 % in 4% steps in all three series.

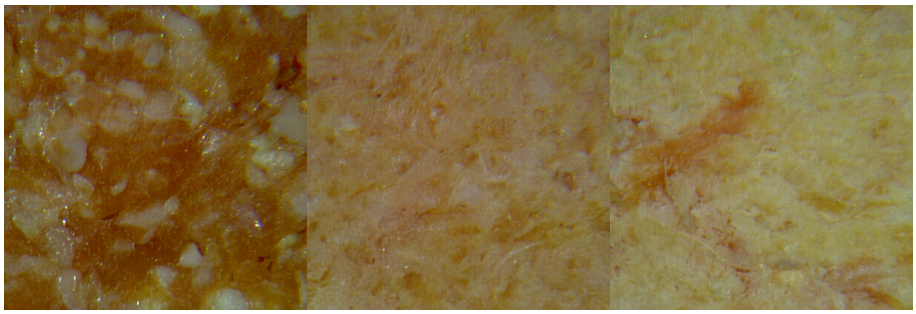

Figure 13. Bovine meat with incrementally added fat. From left to right: 21%, 33% and 41%. SILVACAM false colours.

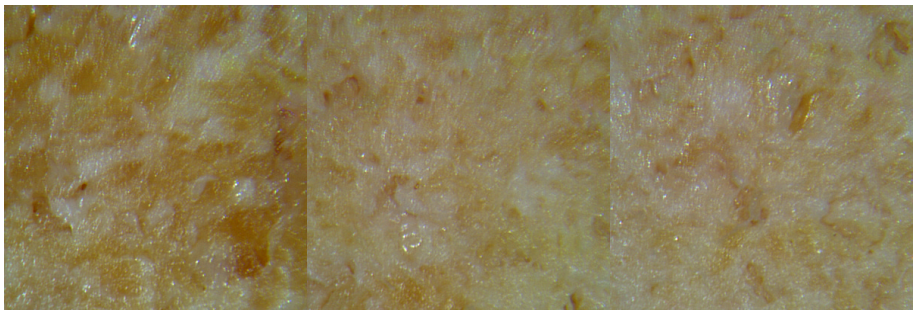

Figure 14. Pork with incrementally added fat fractions. From left to right: 22%,34% and 42% fat. SILVACAM false colours.

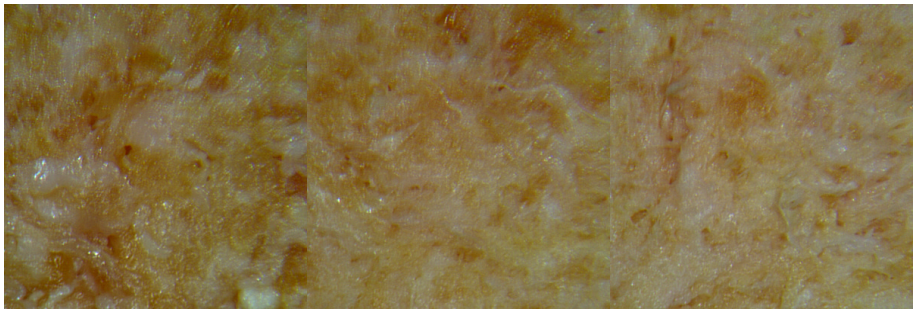

Figure 15. (Pork and bovine) with incrementally added fat. From left to right: 22%, 34%, and 42%. SILVACAM false colours.

Representative 150g samples were taken at the outlet of the IDE-CON mixer (full cross-sectional sampling) after identical mixing times (1 minute) for each new added fat-content increment of 4%. Samples were transported in glass petri-dishes, Figure 16, directly to our laboratory imaging setup presented below, Figure 17 with less than 20 minutes duration. There were no transportation segregation or similar in this type of mixture samples due to the extremely high viscosity of the meat-fat mixtures.

Figure 16. Petri-dishes with meat/fat mixtures. From top to bottom: Bovine, Bovine/Pork, Pork and pure fat. Fat content increases from left to right. Glass covers were removed just prior to imaging.

IMAGING SYSTEM

All studies reported here used a trusted, old-time friend of the Applied Chemometrics Research Group, the "SILVACAM" NIR/R/G digital camera (modified from an original JVC R/G/B television camera by the now defunct Finnish "Karelsilva" company (B. Braam). Figure 17 below presents the laboratory SILVACAM set-up.

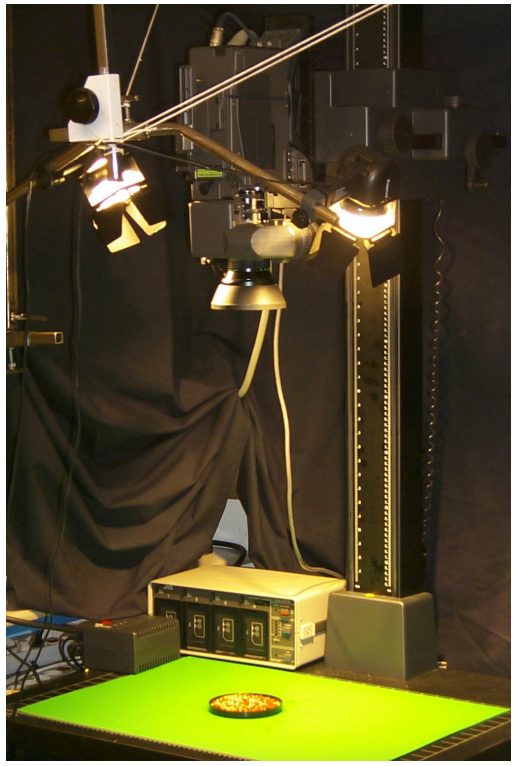

Figure 17. The SILVACAM imaging system at ACRG. Modified JVC-camera, with two quasi-parallel 150W illumination sources. Sampleholder (round) on sample table.

All image analysis systems are critically dependent upon a *proper* illumination system, which we have commented upon in several of our earlier powder and mixture studies[2-6]. Sometimes the AMT-derivation is directly dependent upon a unilateral low-angle illumination for example, while for other characterisations uniform multi-source illumination fits the bill. Each image analysis characterisation problem in fact always necessitates a thorough initial analysis of the proper illumination requirements for example. We shall here refrain from further commenting on this fundamental problem as all the examples used have been subjected to careful illumination optimisation efforts.

RESULTS

Results from applying the alternative AMT and MIR$^+$ approaches on the ten different data sets introduced above will be presented in parallel below. Focus is on *comparing* the optimal multivariate calibration models produced for each individual case; thus we performed *individual* multivariate calibration outlier screenings, and model-dimensional validations etc. for each model. For precisely this type of relative comparison purposes *full cross-validation* comes to its right with full force [7]. All models were calibrated against the pertinent mixing fraction as $\mathbf{y_1}$ variable (PLS1), while the relevant AMT-spectra or the alternative MIR$^+$-spectra served as the X-data block.

The number of objects (images) and replicates are equal in MIR$^+$ and AMT, but the pretreatment used wary in the examples. In some cases all replicates are shown (Figure 18 left), while in other cases replicate-spectra have been *averaged* (Figure 18 right), resulting in fewer objects in the model.

All AMT-spectra have been centered and scaled to uniform standard deviation (*auto-scaled*). In some MIR$^+$ cases, scaling the data can blow up noise and is thus avoided where possible. In other cases though, scaling the MIR$^+$ histograms was found a necessity.

Two-component Granular Mixtures

Black Pepper and White PVC

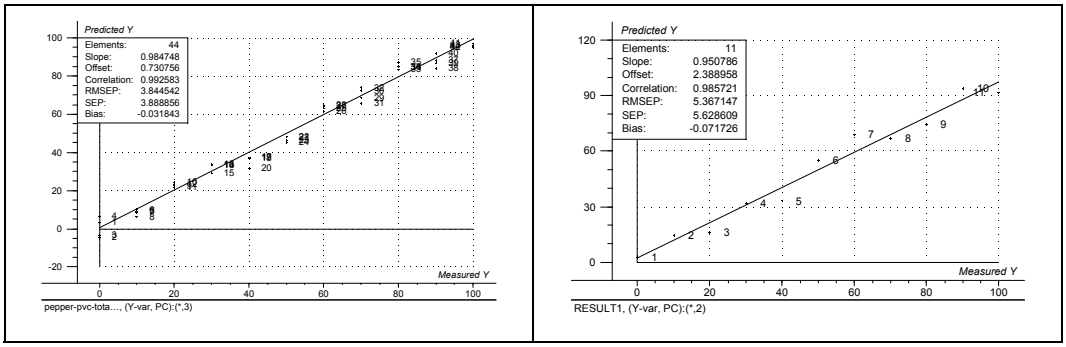

Figure 18. Black Pepper and PVC Pread-Meas plots. Left: MIR$^+$, Right: AMT

	# Comp	Slope	Offset	Correlation	RMSEP
MIR$^+$	3	0.985	0.731	0.993	3.845

AMT	2	0.951	2.389	0.986	5.367

In the high-contrast ("easy") black pepper vs. white PVC-pellets case, MIR$^+$ performs *slightly* better with one additional component (fully significant according to the validation) is used.

This is one example where scaling is applied to the MIR$^+$ histogram. The predicted images are closely to a true black & white (one-bit) image, with information mainly in the beginning and end of the spectra. Scaling the data allows also the middle part of the histograms to influence on the model. Because of the very high contrast between the elements, the current example could possibly also be solved directly with thresholding.

Coriander & White Pepper

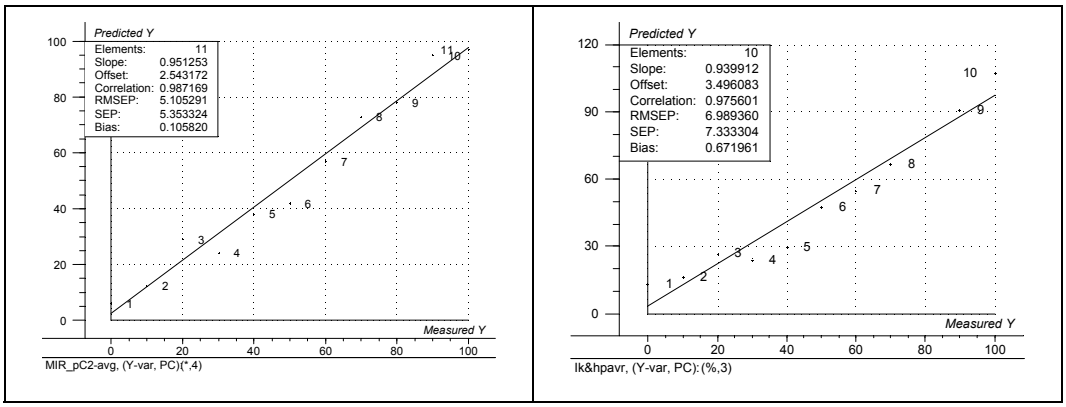

Figure 19. Coriander and White Pepper Pread-Meas plots. Left: MIR$^+$, Right: AMT

	# Comp	Slope	Offset	Correlation	RMSEP
MIR$^+$	4	0.951	2.543	0.987	5.105
AMT	3	0.940	3.496	0.976	6.989

By using one more component, MIR$^+$ shows *marginally* better performance in the "very difficult" coriander vs. white pepper example.

In this example, scaling the MIR$^+$ data was not required. Because there is almost no contrast between the two classes, this example is not solvable using thresholding; a more subtle approach is required, hence MIR$^+$.

Grey and White PVC-pellets

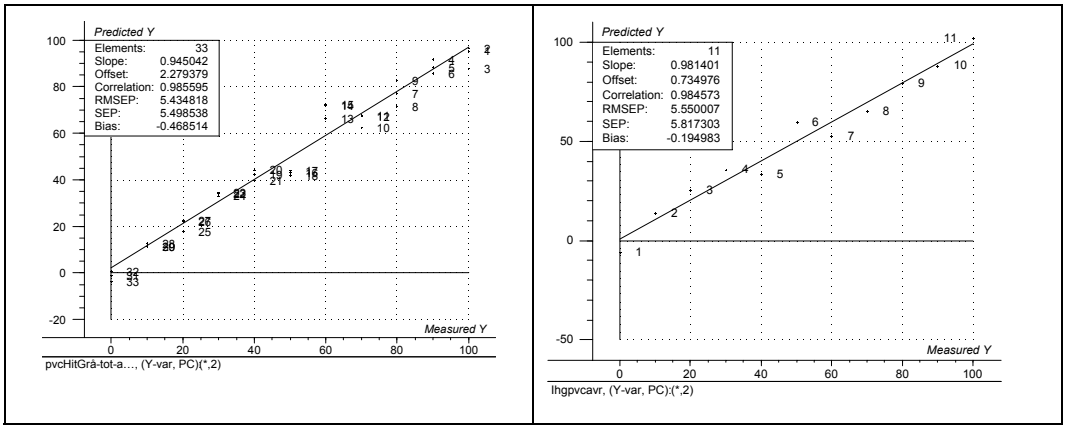

Figure 20. Grey and White Pread-Meas plots. Left: MIR^{+}, Right: AMT.

	# Comp	Slope	Offset	Correlation	RMSEP
MIR^{+}	2	0.945	2.279	0.986	5.435
AMT	2	0.981	0.735	0.985	5.550

In the case of the grey and white PVC-pellets the results are practically equal, although here AMT displays a clearly more comfortable slope (of a *fitted* "predicted vs. measured" regression).

This is another example of high spectral contrast, especially in the predicted images. Again, the data was scaled to extract information also from the middle parts of the histograms.

Grey PVC-pellets and green beans

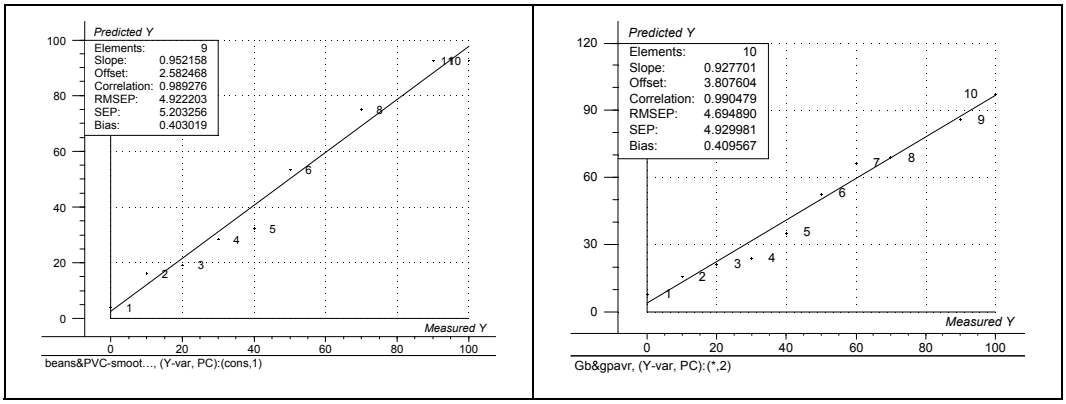

Figure 21. Grey PVC-pellets and green beans Pread-Meas plots. Left: MIR+, Right: AMT.

	# Comp	Slope	Offset	Correlation	RMSEP
MIR+	1	0.952	2.582	0.989	4.922
AMT	2	0.928	3.807	0.991	4.695

MIR+ has a slightly better performance in the grey PVC-pellets/green beans example, considering it uses less components.

In this example, the MIR+ histograms were not scaled. There is only small contrasts between the two elements, and the model uses the major "shape" of the histogram, and not so much the intermediate variables.

Three-Component Granular Mixture

PLS1 (y_1 : Peas mixing fraction)

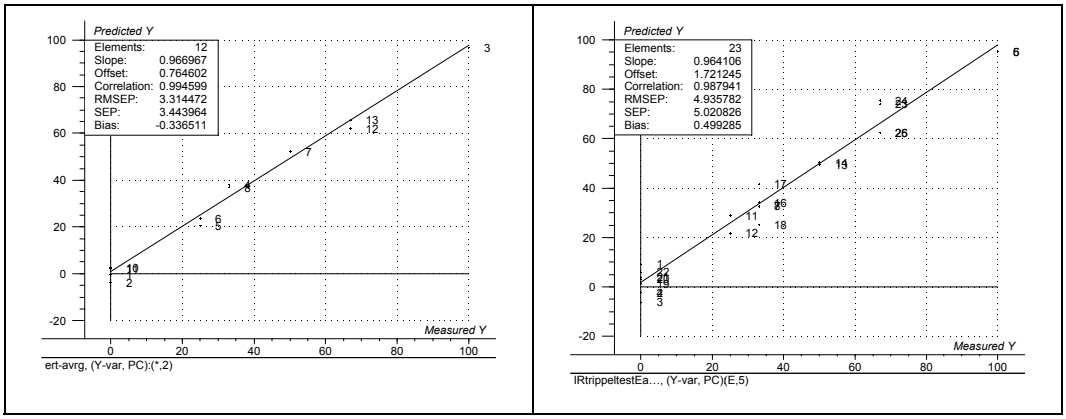

Figure 22. 3-component mixture modelled for Peas. Pread-Meas plots. Left: MIR+, Right: AMT.

	# Comp	Slope	Offset	Correlation	RMSEP
MIR+	2	0.976	0.716	0.992	3.866
AMT	5	0.964	1.721	0.988	4.936

Concerning pea mixing fraction predictions, MIR+ is clearly performing best, using two components vs. AMT which uses five.

In none of the three cases involving three-component mixtures, scaling were applied to the MIR+ data. In the plots above (Figure 22), notice that the number of elements differ by a factor two. This is due to the use of a different averaging factor in the MIR+ and AMT models. Final comparison is not hampered by this.

PLS1 (y_1 : Maize mixing fraction)

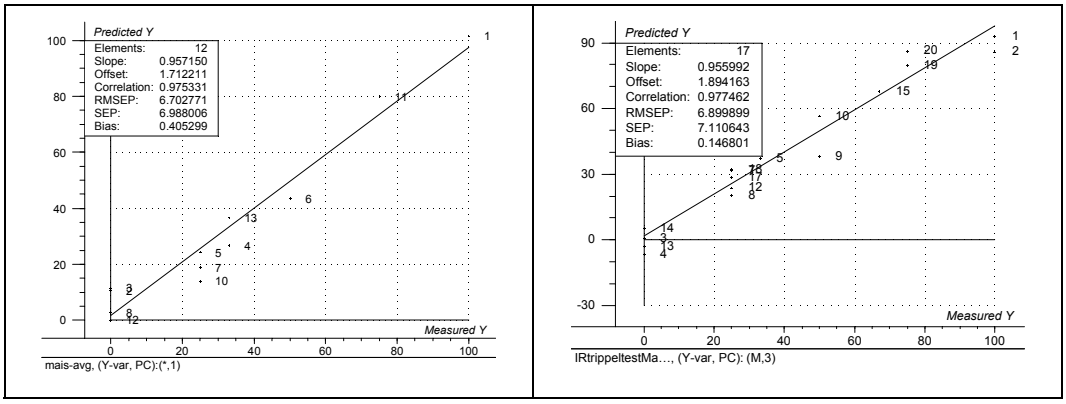

Figure 23. 3-component mixture modelled for Maize. Pread-Meas plots. Left: MIR$^+$, Right: AMT.

	# Comp	Slope	Offset	Correlation	RMSEP
MIR$^+$	1	0.957	1.712	0.975	6.703
AMT	3	0.956	1.894	0.977	6.900

The maize prediction is difficult in both cases, and the results are almost identical. For maize both estimates of RMSEP are the largest of all three vegetables. The only difference is that MIR$^+$ uses one component, while AMT uses three.

PLS1 (y_1 : Carrot mixing fraction)

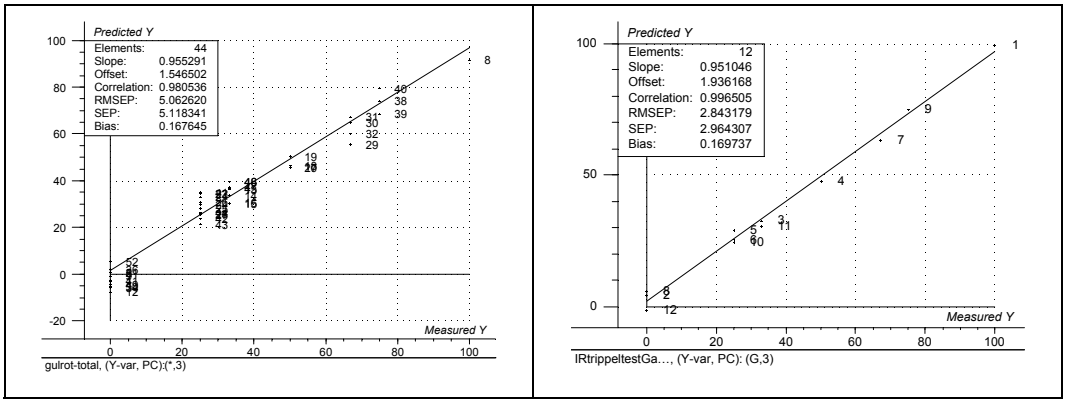

Figure 24. 3-component mixture modelled for Carrots. Pread-Meas plots. Left: MIR$^+$, Right: AMT.

	# Comp	Slope	Offset	Correlation	RMSEP
MIR$^+$	3	0.955	1.546	0.981	5.063
AMT	3	0.951	1.936	0.997	2.843

In the carrot example AMT performs significantly better. The number of components are equal. Carrot cubes are clearly of a significantly different shape than either peas or maize.

Minced Meat

This example is organised in much the same way as the two above. MIR$^+$ training images, (Figure 5) were acquired for 100% pure meat of the relevant types and pure fat respectively, while in the experimental mixtures fat in the range of approx. 20-40% is studied, which is in the representative industrial production range. Meat was calibrated against a black Y-image, and fat calibrated against a white *ditto* (compare Figure 5). Starting at the reference minimum fat-content at 21%, the 4% fat increments (v/v) were added successively in a standardised manner and three replicate-samples were removed for each fat-level. For *each of these parallel physical replicates*, three images-replicates were also acquired by rotating the sample container 120 deg. in front of the camera. Thus there were a total of nine images representing each fat-level; there were overall six fat-levels in total, wiz. 21%, 25%, 29%, 33%, 37% and 41%.

Bovine

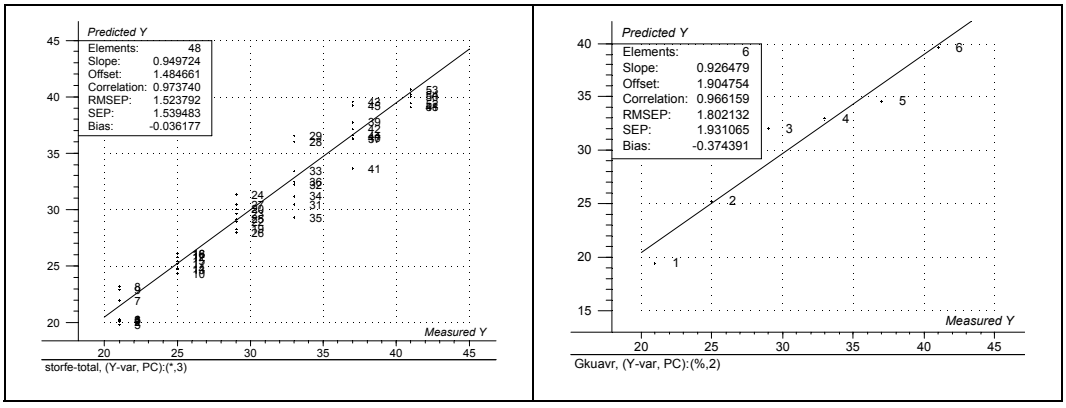

Figure 25. Minced Bovine meat and fat Pread-Meas plots. Left: MIR$^+$, Right: AMT.

	# Comp	Slope	Offset	Correlation	RMSEP
MIR$^+$	3	0.950	1.485	0.974	1.524
AMT	2	0.926	1.905	0.966	1.802

MIR$^+$ predicts the fat content in Bovine meat slightly better, using one more PLS-component.

Pork

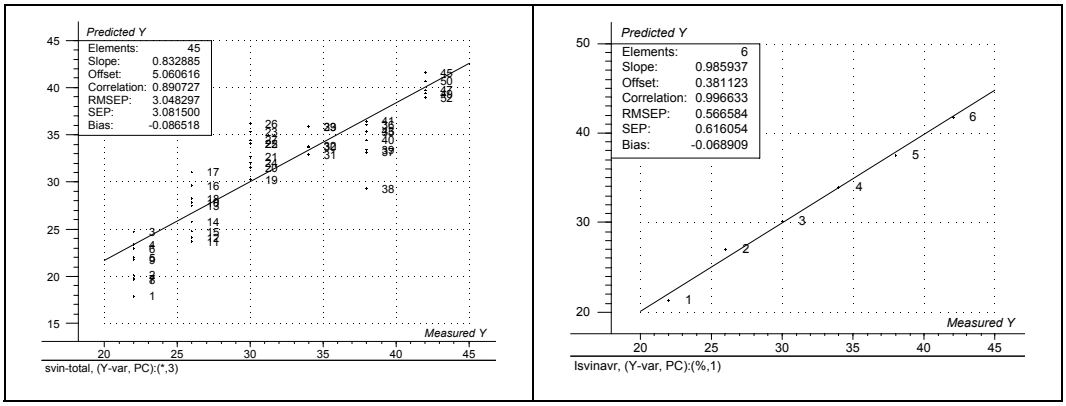

Figure 26. Minced Pork meat and fat Pread-Meas plots. Left: MIR$^+$, Right: AMT.

	# Comp	Slope	Offset	Correlation	RMSEP
MIR$^+$	3	0.833	5.061	0.891	3.048
AMT	2	0.986	0.381	0.997	0.566

In the pork example AMT performs significantly better, also boasting fewer PLS-components.

Bovine & Pork

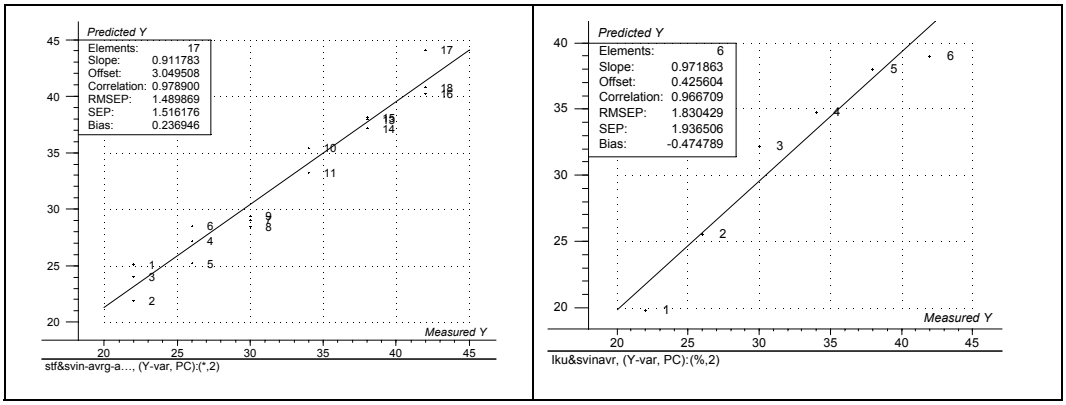

Figure 27. Minced Bovine & Pork meat and fat Pread-Meas plots. Left: MIR+, Right: AMT

	# Comp	Slope	Offset	Correlation	RMSEP
MIR+	2	0.912	3.050	0.979	1.490
AMT	2	0.972	0.426	0.967	1.830

In the combined meat (bovine and pork) vs. fat example, the results are practically equal, except w.r.t. the slope of the fitted regression index; this makes AMT a potential marginal winner here.

Discussion

Two-component mixtures - overview of results:

Essentially all models for both AMT and MIR+ perform satisfactorily in this first overview, but the MIR+ models do perform best, or marginally best, in three out of four detailed evaluations of the selected dry two-component mixture fraction prediction studies; one medium contrast ("somewhat difficult") case has AMT as best. It is encouraging that both the AMT - as well as the MIR+ models essentially both are up to the complicated image analysis job set up. The kinds of precisions obtained in these first attempts are satisfactory: For all models the total span of validation-estimated RMSEP ranges 3.845 - 7.866, while this range for the *best four models* corresponds to: 3.845 - 5.550. Based on an average mixing fraction of 50% these latter correspond to precisions of 7.7% - 11.1% respectively (rel. %). The better end of this interval comprise very respectable precisions for our first attempts image analysis approaches (irrespective of whether one chooses to improve on the MIR+ - or the AMT

approaches; a rational choice demands a much larger factual results data base than the one presently presented). It should be pointed out that the selected two-component mixing systems deliberately includes both the supposedly easiest - as well as the supposedly most difficult systems; also we were certainly surprised e.g. by the unexpected success of the coriander - white pepper case. The complete study of representative dry two-component mixing systems is far from finished at present, and shall be reported on in its totality at a later occasion. The present results can only be characterised as very *encouraging* as feasibility studies go.

Three-component vegetable mixtures:

Winners are about equal, wiz. one AMT- and one MIR$^+$ model, and one draw (maize). Validation estimates of RMSEP are - peas: 3.866 (MIR$^+$); maize: 6.703 (MIR$^+$/AMT); carrots: 2.843 (AMT), which translates to the following rel. % precision (+/- 1 RMSEP) - peas: 7.7%; maize: 13.4% and carrots: 5.7% respectively (all calculated w.r.t. an average mixing fraction of 50% (abs.). Two of these three models, characterised by very realistic sample preparation variances, actually reach *below* industry's precision demand of 8% already from these *first pilot studies* (sic). Clearly the troublesome maize prediction can be better handled by a simple *constant sum* difference calculation! We term these pilot results as *absolutely satisfactory*.

Minced meat mixtures:

For the three best minced meat models, the validation RMSEP estimates translates to 4.9% (MIR$^+$), 1.8% (AMT) and 5.9% (AMT) respectively (all expressed as relative %), compared to a product fat specification range of 21-41% (rel. % calculated w.r.t. an average of 31%). For a first pilot study of this relatively complex on-line mixing system, precisions of 2-6 rel. % can only be characterised as *excellent.* Not only are the outlet sampling procedures not fully optimised yet, neither are the imaging illumination conditions etc. At this time it is only possible to say that there is certainly a significant *potential* improvement to be gained here.

AMT or MIR$^+$:

If judgement would have to passed on the basis of the present results alone, the new, extended MIR$^+$ approach merits very close attention. The degree of accuracy and precision obtained for the present *three very different sets of mixing systems* is impressing indeed. And AMT is a very close runners-up, which should also be related to its recent history of well-documented successes, reported in several complementary

powder/granular matter studies [2-5], in which AMT has shown similar degrees of promising results. Thus we are not at all in a(ny) position to even try to chose between these two powerful chemometric image analysis processing alternatives - on the contrary: they will of course be extensively further explored in parallel.

The above discussion has presented more than enough evidence to leave this pilot study in a very optimistic state. Much interesting real-world, industrial implementation work awaits, as well as an enticing fundamental science, broad-scoped functional powder mixing laboratory study - all with exciting potentials for industrial applications and economic benefits.

Interpretations of alternative model structures: MIR$^+$ vs. AMT

We end this study by showing what kind of detailed interpretations is made possible by systematic evaluation of the prediction models established. By focusing on the final *validated* prediction results, we now examine the models from the perspective of their comparative *intrinsic data structures*, as represented by their loading-weight relationships.

At the same time we shall also honour the inter-comparison objective between AMT and MIR$^+$, although the conclusions above would appear to rule out any unambiguous winner. Thus this comparison shall mostly focus on the basic differences experienced in their respective w-relationships. These two fundamentally different approaches to quantification of mixture – and texture features will necessarily lead to very different loading-weight spectra (they are *de facto* modelling quite different features) – while in the final assessment they may well lead to almost identical prediction strengths, as indeed demonstrated above.

Figure 28 shows the necessary interpretation background in the form of a small recap of the raw images and their corresponding MIR$^+$ and AMT raw spectra respectively. This juxtaposition will make it easy to appreciate the following interpretations.

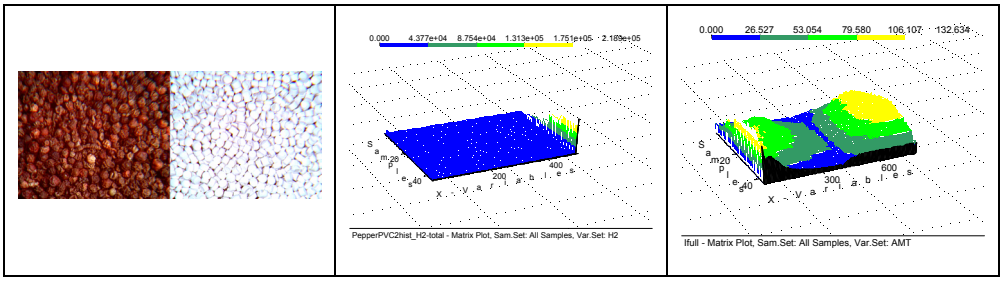

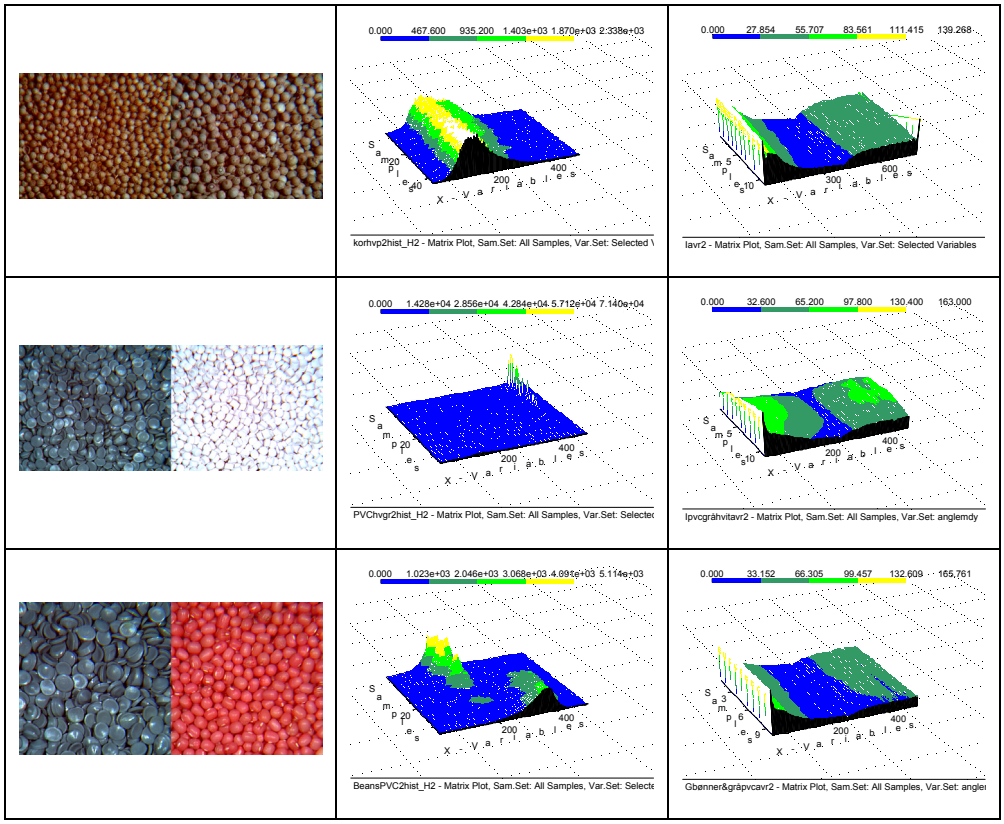

Figure 28. Data presentation of raw data (left), MIR^{+} histograms (middle) and AMT-spectra (right).

Figure 28 shows a two-fold division in high-contrast (row A and C) and intermediate-contrast mixing systems (row B and D). Individual MIR^{+}-modelling lead to the use of *auto-scaled* models for the former, while the latter were best serviced without. One observes the very marked different raw MIR^{+}-spectra for these opposing systems.

These observations makes for easy detection of a similar pattern in both the MIR^{+} and the AMT w-spectra below in Figure 29.

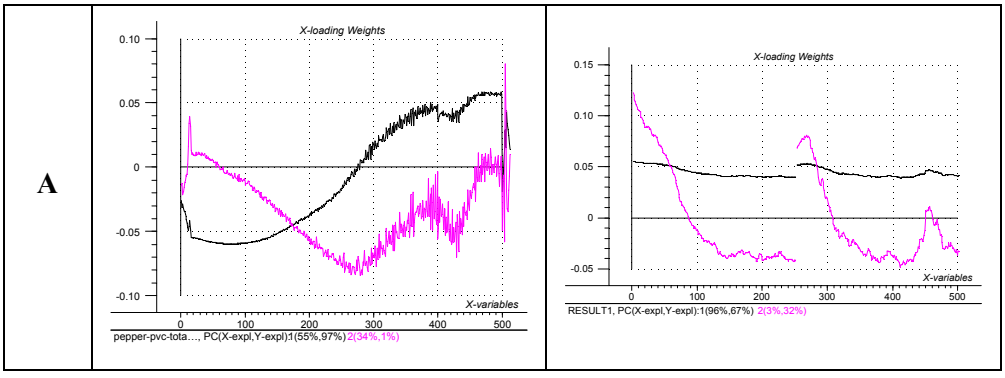

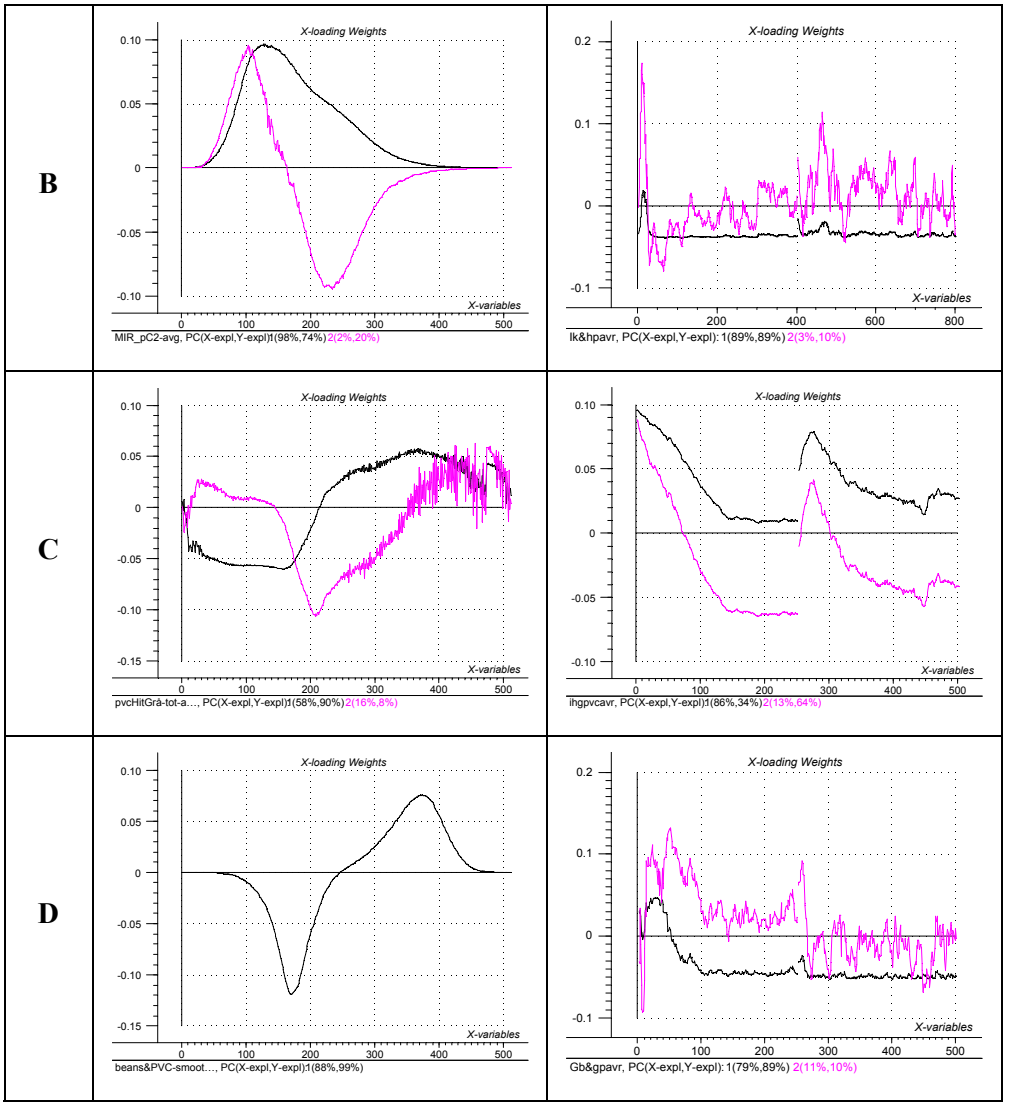

Figure 29. 2-component mixture loading weight plots. Left: Mir$^+$, right: AMT. From top to bottom: Pepper/PVC, Coriander/White Pepper, white/grey PVC and Beans/PVC.

MIR$^+$:

MIR$^+$-modelling of the *intermediate-contrast systems* are distinctive (row B and D). The first PLS-component, to a large extent, takes good care of the Y-modelling but with a very significant *addition* from PLS-component 2 (row B). For both systems w_1 mimics the raw MIR$^+$-spectrum to a very high degree, while the second order *addendum* from PLS-component 2 attest to a slight shift in the X-variable direction for the coriander-white pepper system (row B); for row D system there is an even simpler relationship with mixing fractions (Y) leading to only one significant PLS-component.

For the more-simple-to-model *high-contrast systems* (row A and C) one observes that two PLS-components are also needed, but with only marginally improved Y-variances for the second PLS-component (only first significant according to the validations). It will be appreciated that the X-variance is utilised in a very effective fashion caused by the auto-scaling.

AMT:

For AMT one observes a distinctly opposite pattern. For both high-contrast systems (row A and C) there is now a very marked need for both PLS-components in order to do the prediction modelling effectively (32% and 64% Y-variance accounted for respectively by the second component). Both components are now *highly significant* according to the validations. For both systems, their respective w_1- and w_2-spectra shows essentially the same pattern (rare!), while for the opposing intermediate-contrast systems (row B and D) there is only a small (10%) Y-variance addendum from w_2.

With due reference to the rather disparate four systems some underlying systematics may perhaps be found. MIR$^+$ manages to combine most of the essential X-variance in just one PLS-component (three out of four systems), while AMT would appear to favour two-component systems, especially for the high-contrast cases. Our initial classification into H, I and L-contrast systems may very well be further refined a.o. also based upon this kind of systematic modelling of all systems in the background study (nine systems covering the H, I, L-domain more fully).

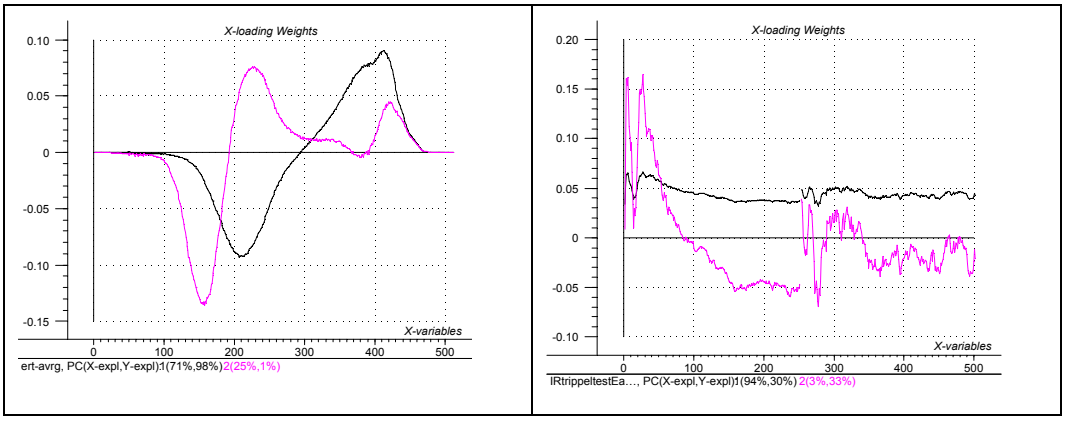

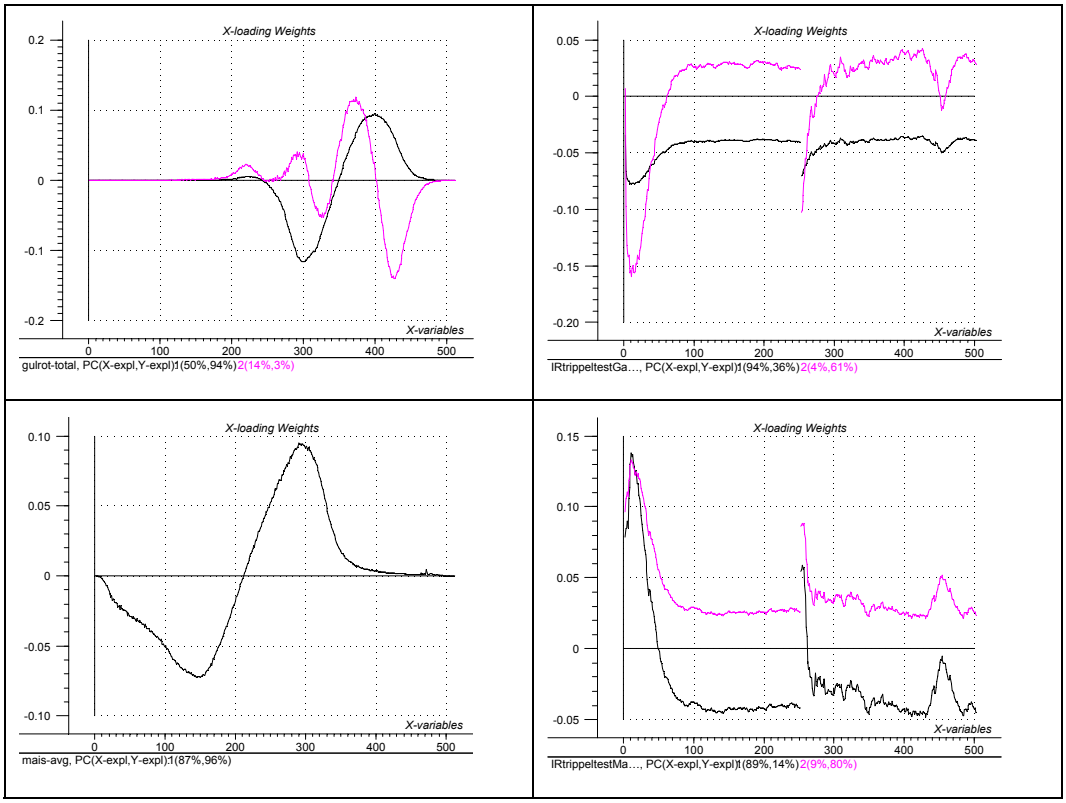

Figure 30. 3-component loading weights plots. Left: MIR$^+$, right: AMT. From top to bottom: Peas, Carrot and Maize.

For the three-component vegetable system we may use the above interpretation systematics in order to simplify what would *appear* to be a more complex issue.

Inspection of Figure 30 again reveals an extremely simple relationship for MIR$^+$ however. For both peas, carrot as well as maize prediction models, the first PLS-component accounts for 98%, 96% and 94% Y-variance respectively, with barely significant, very minor additions for the second components, a very clear one-component trend.

In stark contrast to this, the AMT-relationships show marked multi-component features, some using even more than two validated components, thus further contributing to the overall MIR$^+$ vs. AMT relative pattern. MIR$^+$ is able to model even these, clearly more complex systems, still basically using only one PLS-component – no doubt primarily due to its underlying dichotomous 0/100 model-definition. AMT on the other hand, while able to reach essentially identical prediction validation results, does this in a distinctly more elaborate fashion in which several essential *contrast phenomena* are found distributed over more PLS-components.

The remaining meat-fat systems (Figure 31 below) are no doubt one order of magnitude more complex still. But here again for MIR$^+$ we find the exact same dispositions as for the vegetable – and the dry powder systems both: extreme reliance on the first PLS-component accounting for 88%, 98% and 93% Y-variance respectively, while AMT here shows especially complex multi-component patterns, also between the different meat-fat mixing series internally. In fact there would appear to be very interesting detailed interpretation possibilities for this latter system as regards these internal AMT differences, which we shall never-the-less leave for an other occasion since the overall *comparative* MIR$^+$ vs. AMT pattern remains the same for this system as for the two above:

Considering the gamut of all the three pilot studies, covering a broad swath of relevant real-world, industrial mixing two-component and three-component end-member systems, the overall conclusion would now appear to have become clear:

MIR$^+$ can do with few – what AMT must do with more.

Following Occam's razor, we then must point to MIR$^+$ as a very powerful new complement to AMT in the family of multivariate image regression problem-dependent pre-processing facilities, which we intend to develop much further with great interest.

AMT on the other hand, confirms its status of being able to model even very complex systems with a detailed internal model structure, well suited for in-depth interpretations.

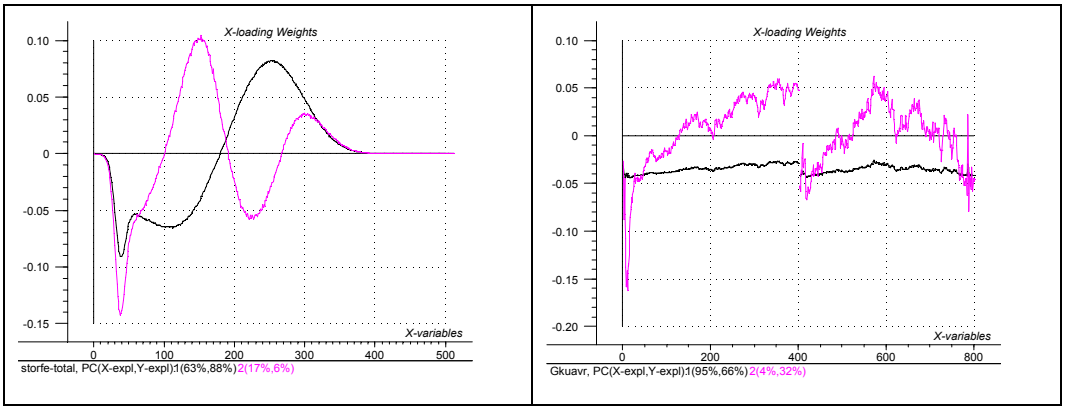

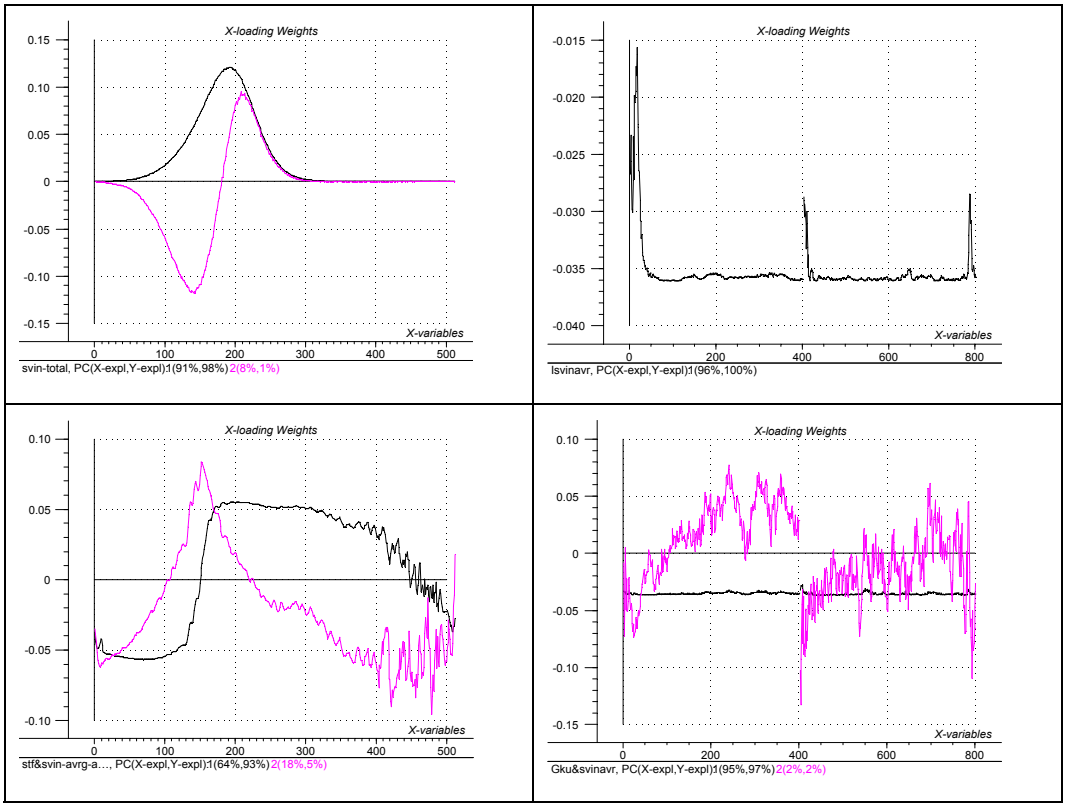

Figure 31. Minced Meat loading weight plots. Left: MIR⁺, right: AMT. From top to bottom: Bovine, Pork and Bovine+Pork.

ACKNOWLEDGEMENTS

Ide-Con was founded 1989 and has been granted three patents on new mixing concepts. The mixer has been tested out at the Powder of Science and Tecnology (POSTEC), Porsgrunn Norway as well as in several key industries. We are very greatful to Geir Nordahl and Thor Ragnar Hem for permission to publish results here based on our first collaboration using IC-B13.

REFERENCES

[1] T. Shinbrot and F. J. Muzzio, *Nonequilibrium Patterns in Granular Mixing and Segregation.* Physics today, **53/3**. (2000) pp 25-30

[2] J. Huang and K.H. Esbensen, *Applications of AMT (Angle Measure Technique) in Image Analysis Part I. A New Methodology for in-situ Powder Characterization.* Chemometrics and Intelligent Laboratory Systems. **54/1**. (2000) pp 1-19

[3] Jun Huang and Kim H. Esbensen . *Applications of AMT (Angle Measure Technique) in Image Analysis PART II: Prediction of Powder Functional Properties and Mixing Components using Multivariate AMT Regression (MAR).*, accepted by Chemo. Lab. 2000.

[4] J. Huang, B. Møller, K.H. Esbensen, L. Munck, *Characterization of Barley Germination Process from the Images by Combined AMT(Angle Measure Technique) Chemometric Analysis*. Submitted for publication in Analytica Chimica Acta, 2000

[5] K.H. Esbensen and J. Huang, *High sensitivity particulate impurity detection and quality control by unfolded image AMT.* Submitted for publication in Journal of Chemometrics, 2000

[6] J. Huang and K.H. Esbensen, *Methodology Development and Applications of Multi-way methods in Image Analysis.* Submitted for publication in Journal of Chemometrics, 2000

[7] K. Esbensen et.al. *Multivariate Data Analysis –in practice, 4th edition.* (2000) CAMO ASA, Oslo, Norway. ISBN 82-993330-2-4.

[8] P. Geladi and K. Esbensen. *Regression on multivariate images: Principal Component Regression for modelling, prediction and visual diagnostic tools.* J. of Chemometrics **5** (1991) 97-111.

[9] K. Esbensen, P. Geladi and Hans Grahn. *Strategies for Multivariate Image Regression.* Chemo. Lab. **14** (1992) 357-374.

[10] P. Geladi and H. Grahn. *Multivariate Image Analysis.* (1996). John Wiley and Sons, Chichester, UK pp. 316

[11] F. Lindgren, P. Geladi and S. Wold. *The Kernel Algorithm for PLS.* J. of Chemometrics, **7** (1993) 45-59.

[12] S. Wold, H. Martens and H. Wold. *The multivariate Calibration problem in chemistry solved by the PLS method*. (1983) Proc. Conf. Matrix pencils, (A. Ruhe, B. Kågstrøm, eds), March 1982. *Lecture Notes in Mathematics,* Springer Verlag, Heidelberg, 286-293

[13] H. Martens and S.Å. Jensen. *Partial Least Squares regression: A new two-stage NIR calibration method.* (1983) Proc. 7th World Cereal and Bread Congress. Prague June 1982. (Holas and Kratochvil, eds.) Elsevier Publ., Amsterdam, 607-647.

[14] H. Martens and T. Næs. *Multivariate Calibration.* (1989). John Wiley & Sons Ltd. Chichester, UK. ISBN 0 471 90979 3 pp. 419

[15] T.T. Lied, P. Geladi and K. Esbensen. *Multivariate Image Regression (MIR): implementation of image PLSR – first forays*. J. Chemometrics, **14** (2000) pp. 585-598

[16] T.T. Lied and K. Esbensen. Principles of MIR, Multivariate Image Regression I: regression typology and representative application studies. (Submitted for publication).

[17] T.T. Lied and K. Esbensen. *Principles of MIR, Multivariate Image Regression II: Cross Validation – what you see is what you get.* (Submitted for publication, 2000).

[18] R. C. Gonzalez and R. E. Woods. *Digital Image Processing.* (1993) Addison-Wesley Publishing Company, Inc. Reading, USA. ISBN 0-201-60078-1 pp. 716.